AIP | Journal of Applied Physics

Coexistence of intrinsic and extrinsic origins of room temperature ferromagnetism in as implanted and thermally annealed ZnO films probed by x-ray absorption spectroscopy

P. Satyarthi, S. Ghosh, B. Pandey, P. Kumar, C. L. Chen, C. L. Dong, W. F. Pong, D. Kanjilal, K. Asokan, and P. Srivastava

Citation: Journal of Applied Physics **113**, 183708 (2013); doi: 10.1063/1.4804253
View online: http://dx.doi.org/10.1063/1.4804253
View Table of Contents: http://scitation.aip.org/content/aip/journal/jap/113/18?ver=pdfcov
Published by the AIP Publishing

Coexistence of intrinsic and extrinsic origins of room temperature ferromagnetism in as implanted and thermally annealed ZnO films probed by x-ray absorption spectroscopy

P. Satyarthi,[1] S. Ghosh,[1] B. Pandey,[2] P. Kumar,[3] C. L. Chen,[4] C. L. Dong,[5] W. F. Pong,[6] D. Kanjilal,[3] K. Asokan,[3] and P. Srivastava[1,a)]
[1]*Nanostech Laboratory, Department of Physics, Indian Institute of Technology Delhi, Hauz Khas, New Delhi 110016, India*
[2]*School of Applied Sciences, Gautam Buddha University, Greater Noida 201310, Uttar Pradesh, India*
[3]*Inter University Accelerator Centre, Aruna Asaf Ali Marg, New Delhi 110067, India*
[4]*Institute of Physics, Academia Sinica, Taipei 11529, Taiwan*
[5]*National Synchrotron Radiation Research Center, Hsinchu 30076, Taiwan*
[6]*Department of Physics, Tamkang University, Tamsui 251, Taiwan*

(Received 8 March 2013; accepted 22 April 2013; published online 10 May 2013)

The present work reports the structural and ferromagnetic properties of 200 KeV Ni^{2+} ion implanted ZnO films before and after annealing at 650 °C in air and correlates these properties with their electronic structures. X-ray absorption spectroscopy (XAS) at Zn and Ni K-edges reveal that Zn metal cluster is absent in ZnO matrix, but there is an indication of clustering of Ni metal as a secondary phase. The XAS analysis of O K-edge shows (i) non-stoichiometric NiO segregation in as-implanted film and its absence/reduction in air annealed film, (ii) partial substitution of Ni^{2+} ions at tetrahedral Zn sites, and (iii) presence of lattice defects such as oxygen vacancies in both films. The observed ferromagnetic behavior of as-implanted and air annealed films has both intrinsic as well as extrinsic origins. The intrinsic and extrinsic origins are discussed in terms of bound magnetic polaron model and presence of antiferromagnetic NiO phase/ferromagnetic Ni metal clusters, respectively. © *2013 AIP Publishing LLC*. [http://dx.doi.org/10.1063/1.4804253]

I. INTRODUCTION

Spintronics aims to fabricate semiconductor devices using both electron and spin polarized carriers. Dilute magnetic semiconductors (DMSs) with room temperature ferromagnetism (RT-FM) are considered as one of the most promising materials for spintronics technologies.[1] Transition metal (TM) doped zinc oxide (ZnO) is one such DMS system that has been extensively investigated both by theoretical and experimental research groups predicting ferromagnetic behavior at low and high (RT and above) temperatures.[2–5] However, there is continuous debate regarding the origin of FM and role of TM in such systems. Some studies[6,7] indicate that the origin of FM is intrinsic in nature and is due to exchange interaction between delocalized charge carriers and localized magnetic moment of TM ion. However, in some cases,[8,9] it is reported that FM is extrinsically originated from segregation of TM as metallic phase or from secondary magnetic phase. Defect densities, such as oxygen/zinc vacancies or interstitials[10,11] and cluster of oxygen vacancies[12] can alone trigger FM in ZnO without TM doping. In case of Ni doped ZnO films, several interpretations on RT-FM exist in the literature. Liu *et al.*[13] reported that RT-FM in ZnO for Ni concentrations (2%, 4%, and 7%) is intrinsic and for 11% Ni concentration ferromagnetism is extrinsic in nature due to precipitation of Ni. However, there are some reports where no ferromagnetism was observed in ZnO:Ni films.[14] In order to further explore the mechanism of FM in such complex magnetic materials, researchers have adopted advanced synchrotron-based x-ray absorption spectroscopy (XAS) for probing electronic structure of TMs.[15–17] The recent XAS studies reveal that Ni ion implanted ZnO films[17] and Ni doped ZnO nanorods[18] show intrinsic RT-FM mediated through oxygen vacancy related native defects. The stability and reproducibility of RT-FM in Ni doped ZnO in various environments are one of the most challenging issues for device application in spintronics. It has been reported that the nature of FM in Ni doped ZnO does not remain intrinsic upon annealing in various environments at high temperature because of segregation of TM ions.[19] Singhal *et al.*[20] reported that FM in hydrogenated and vacuum annealed Ni doped ZnO disappears upon long reheating in air at very high temperatures of 700 °C and 800 °C, respectively.

It is desirable that the DMS materials should sustain their ferromagnetic property at relatively high temperatures considering their applications in future devices. However, as defects play a major role in the origin of their FM properties, most of these materials do not retain FM at elevated temperatures. Therefore, it is important to investigate robustness of their FM at higher temperature. The present work originates with this motivation. In order to investigate this issue, Ni ion implanted ZnO/sapphire films were chosen. The RT-FM of these as-implanted films with various Ni concentrations has been reported in earlier studies.[17,21] Present investigations correlate the origin of ferromagnetism in Ni implanted and post annealed ZnO films with their electronic structure probed by XAS.

a)Author to whom correspondence should be addressed. Electronic mail: pankajs@physics.iitd.ac.in.

II. EXPERIMENTAL DETAILS

ZnO thin films of thickness ~800 nm prepared by pulsed laser deposition (PLD) technique were implanted at room temperature with Ni^{2+} ions of energy 200 KeV using the low energy ion beam facility (LEIBF)[22] of the Inter University Accelerator Centre, New Delhi. Implantation fluence of 2×10^{16} ions/cm^2 was used to obtain 7% Ni ion concentration in ZnO matrix, i.e., ZnO:Ni as-implanted thin film. The as-implanted thin film was annealed at 650 °C in air for 6 h hereafter denoted as ZnO:Ni air annealed thin film. The range (~102.3 nm) along with longitudinal straggling (40.6 nm) of 200 KeV Ni^{2+} ions in the film was calculated using the simulation program Transport of Ions in Matter (TRIM).[23] The structural characterization of both films were carried out using X-ray diffraction (XRD) (Philips X'Pert PRO). The magnetic properties of these films were investigated at room temperature using a superconducting quantum interference device (SQUID) magnetometer (MPMS, Quantum design). Electronic structure of both films is probed by X-ray absorption spectroscopy (XAS). The XAS measurements were performed at the National Synchrotron Radiation Research Center (NSRRC) in Taiwan. While the x-ray absorption in near edge structure (XANES) spectra at O K-edge was measured at the high-energy spherical grating monochromator (HSGM) BL20A1 (resolving power $E/\Delta E = 8000$) in ultrahigh vacuum ($<5 \times 10^{-9}$ Torr) in the total electron yield (TEY) detection mode, the Zn and Ni K-edges were measured at the Wiggler beamline.

III. RESULTS AND DISCUSSION

Figure 1 shows the XRD patterns of ZnO:Ni as-implanted and ZnO:Ni air annealed films. The characteristic peaks of the air annealed film are similar to as-implanted film indicating single crystalline wurtzite phase with c-axis orientation. Both films do not show formation of any secondary phase such as crystalline Ni metal or NiO phase.[17] Absence of any crystalline secondary phase(s), within the detection limit of XRD is evident. From conventional XRD, it is difficult to ascertain crystalline Ni metal precipitates if these are crystallographically misoriented inside ZnO matrix.[24] With intense x-ray source, like synchrotron radiation the detection limit can be improved and it is possible to detect these secondary crystalline Ni metallic phase.[25] However, the presence of Ni or its oxide in amorphous phase could not be detected by this technique.

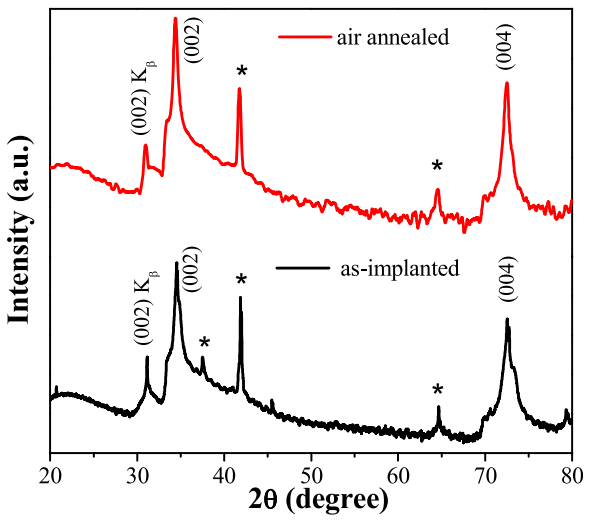

FIG. 1. XRD patterns of ZnO:Ni as-implanted and ZnO:Ni air annealed films. The peaks marked by the symbol (*) correspond to the sapphire substrate. No peaks corresponding to metallic Ni or its oxides are seen.

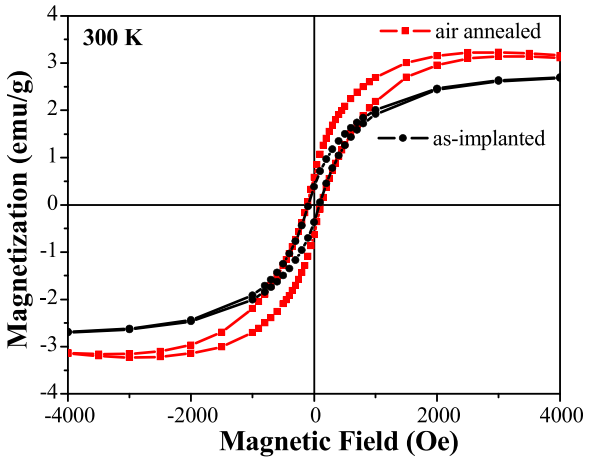

FIG. 2. M-H curves recorded at 300 K corresponding to ZnO:Ni as-implanted and ZnO:Ni air annealed films showing ferromagnetic nature of the films.

The magnetization versus magnetic field (M-H) curves, measured at room temperature for ZnO:Ni as-implanted and ZnO:Ni air annealed films are shown in Figure 2. As evident, there are clear hysteresis loops with finite coercivity (H_c) and remanent magnetization (M_r) indicating their ferromagnetic behavior (see Table I). From Figure 2 and Table I, it is clear that the ferromagnetic contribution is enhanced in air annealed film as compared to the as-implanted film. Saturated magnetic moments for as-implanted and air annealed films are 0.48 and 0.66 μ_B/Ni, respectively. From these measurements, it is not possible to further comment on the origin of RT-FM observed in these films. However, one source may be an existence of secondary phase such as metallic Ni. It should be pointed out here that XRD reveals absence of Ni metal clusters and its secondary oxide phases in crystalline form. Therefore, to get a better insight into the origin of RT-FM in as-implanted and air annealed films, it is essential to investigate their local electronic structure using XANES.[26]

Figure 3 shows the Zn K-edge XANES spectra at room temperature for ZnO:Ni as-implanted, ZnO:Ni air annealed and ZnO thin films. XANES spectra from standard (ST) reference specimens such as ZnO and metal Zn are also shown

TABLE I. Ferromagnetic contribution of ZnO:Ni as-implanted and ZnO:Ni air annealed films showing saturation magnetization M_s, remanent magnetization M_r, and coercivity H_c.

Sample	Saturation magnetization M_s (μ_B/Ni)	Remanent magnetization M_r (μ_B/Ni)	Coercivity H_c (Oe)
As-implanted	0.48	0.07	90
Air annealed	0.66	0.12	116

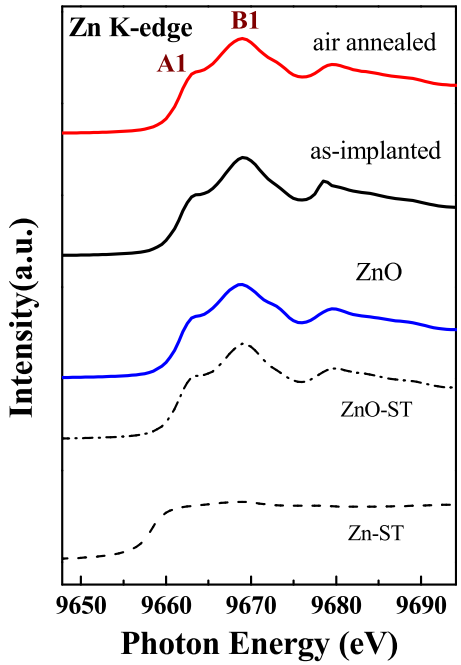

FIG. 3. The experimental XANES spectra recorded at the Zn K-edge in the total electron yield (TEY) detection mode at room temperature for the ZnO:Ni as-implanted, ZnO:Ni air annealed, ZnO thin films (solid line) and standard (ST) reference ZnO, Zn metal (dashed line).

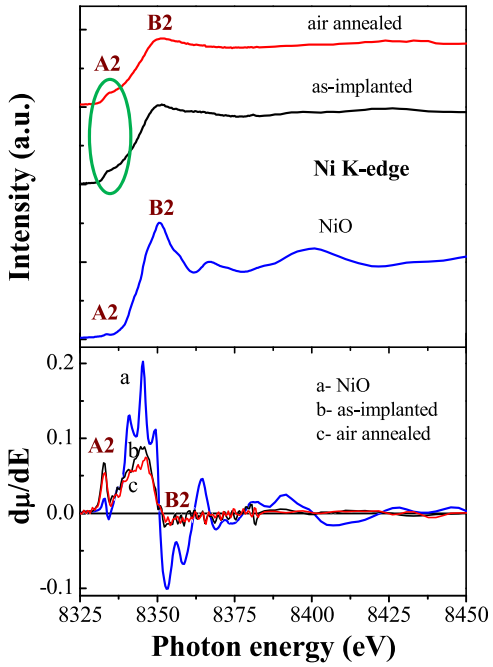

FIG. 4. The experimental XANES spectra recorded at the Ni K-edge in the total electron yield (TEY) detection mode at room temperature for the ZnO:Ni as-implanted, ZnO:Ni air annealed films and reference NiO. The associated derivative spectra for these samples are also presented in lower spectrum.

in the same figure. The features A1 and B1 appearing in the Zn K-edge arise due to electron transition from Zn 1s to unoccupied Zn 4p and thus probes the unfilled electronic density of states (DOS).[27] The overall Zn K-edge spectrum of the air annealed film is similar to that of as-implanted film, ZnO thin film and reference ZnO. Therefore, it can be concluded that Zn related defects such as metallic Zn clusters are not induced due to implantation of Ni ions into ZnO matrix and annealing the as-implanted film at high temperature. Overall, Zn atom environment is same in as-implanted, air annealed and ZnO thin films with a majority of Zn atoms in ZnO wurtzite structure.

Figure 4 shows XANES spectra at Ni K-edge of ZnO:Ni as-implanted, ZnO:Ni air annealed and reference NiO and provide insight on the local electronic structure around Ni ion. Two major features, pre edge peak A2 and main absorption peak B2 are observed in both films.[18,28] A distinct difference of spectral shapes in pre and post edge regions of the films as compared to reference NiO confirms absence of any detectable trace of NiO secondary phase. However, for both films, electronic configuration of Ni was found to be Ni^{2+} from the position of main absorption edge. Pre edge feature (A2), typical for Ni^{2+} is associated with transition of Ni 1s electron to Ni 3d-O 2p hybridized states. It is apparent that the gap between the pre-edge and major onset of absorption starts to fill in these films (see encircled region in the figure) and this filling can be interpreted as conversion of some of the Ni^{2+} ions into metallic Ni.[17,29] The marked difference in plateau like metallic nature of Ni^0 in the films as compared to weak pre-edge feature in NiO is clearly observable in the derivative spectra of Fig. 4. It implies that Ni dopants in ZnO matrix are in mixed oxidation state of Ni^{2+} and metallic Ni^0. The possibility of metallic Ni^0 to form the intermetallic NiZn secondary phase is negligible because Zn K-edge spectra show no shift towards lower energy in both the films, which is expected if NiZn phase is formed.[30] Even the XRD pattern does not show any signature of the presence of crystalline NiZn in the films. In future, detailed extended x-ray absorption fine structure (EXAFS) studies similar to Co doped ZnO thin films[31] will be carried out to further comment on the presence/absence of NiZn secondary phase. However, from the Ni K-edge XANES spectra, it is difficult to quantify the distribution of Ni^{2+} ions at tetrahedral Zn^{2+} site in wurtzite environment or its NiO form and hence observed ferromagnetism in both films cannot be explained solely due to effects of precipitation of Ni metal alone.

The normalized XANES spectra at O K-edge for ZnO, ZnO:Ni as-implanted, ZnO:Ni air annealed films shown in Fig. 5 provide support to understand the role of oxygen in their electronic structure. The ZnO, as-implanted and air annealed films exhibit quite different spectral features which can be interpreted as follows: (a) pre edge peaks A3 (~530.7 eV) and B3 (~532.3 eV) are attributed to O 2p states hybridized with Zn 3d4s and Ni 3d states (b) main absorption peak C3 at ~537 eV refers transition to O 2p states in conduction band (c) peak D3 in region between 538 and 550 eV can be assigned to O 2p sates hybridized with Zn 4p and Ni 4sp states.[32,33] Sharp absorption peak C3 appearing in the spectrum of ZnO is greatly reduced in intensity for as-implanted and air annealed films as a result of Ni substitution at Zn sites.[34] The feature B3 appearing in ZnO thin film is not sharp due to almost completely occupied 3d states. When Ni^{2+} ions substitute for tetrahedral Zn sites in ZnO, an empty Ni 3d impurity band with t_{2g} symmetry is strongly hybridized with O 2p states and may give rise to sharp pre-

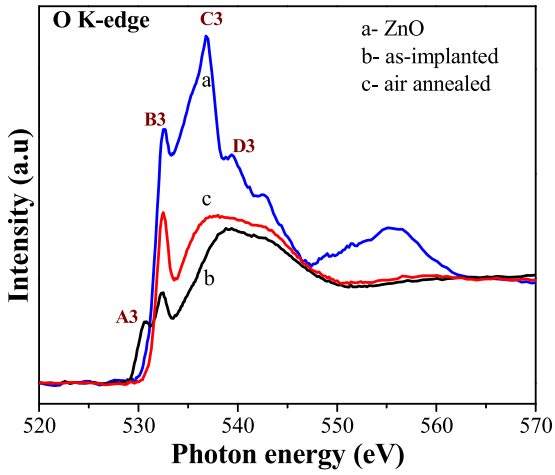

FIG. 5. The experimental XANES spectra recorded at the O K-edge in the total electron yield (TEY) detection mode at room temperature for the ZnO, ZnO:Ni as-implanted and ZnO:Ni air annealed films.

edge peak B3 in as-implanted and air annealed films.[33,34] However for as-implanted film, another weak pre edge feature A3 separated by 1.6 eV from peak B3 is seen. It may be attributed to the presence of non-stoichiometric NiO phase with pyramidal symmetry.[35] Implantation of Ni in ZnO matrix creates point defects such as oxygen deficiency thus favoring the formation of non-stoichiometric NiO with deviation from tetrahedral symmetry. This NiO lacks apical oxygen in octahedral environment (NiO_6) as compared to bulk NiO and there is a splitting of unoccupied e_g states of Ni^{2+} into lower $3d_z^2$ and higher $3d_{x^2-y^2}$ states with separation of 1.5 eV. Therefore, in as-implanted film, pre edge peak A3 arises from O 2p states hybridized with $3d_z^2$ states and pre edge peak B3 has contributions from Ni^{2+} ions substituted at Zn ions in tetrahedral environment as well as from unoccupied $3d_{x^2-y^2}$ states of Ni ions in pyramidal symmetry. The increased intensity of pre-edge peak B3 in air annealed film is due to decomposition of non-stoichiometric NiO into Ni^{2+} ions at high temperature so that these Ni^{2+} of smaller ionic radius (0.69 Å) can substitute the tetrahedral Zn^{2+} ions (0.74 Å) in hexagonal environment. In addition, the broadness of peak C3 is ascribed to presence of oxygen vacancies[33] because oxygen vacancy affects the surrounding shell of oxygen atoms by effectively altering their 1s core level binding energy and hence 1s-2p dipole excitation from these oxygen atoms. The defect density of oxygen vacancies appears similar in the as-implanted and air annealed films as evident by peak C3, but it is large as compared to ZnO film. The activation energy for oxygen diffusion is much larger than Zn and Ni resulting in less oxygen diffusion from air into film.[36] Therefore, on annealing substantial change in oxygen vacancies in as-implanted film is not expected.

Magnetic measurements of ZnO:Ni as-implanted and ZnO:Ni air annealed films reveal two important results: (i) the existence of RT-FM in both films and (ii) enhancement in ferromagnetic contribution of air annealed film. The possibility of ferromagnetic Ni metal clusters examined in Ni K-edge spectra could be thought as an extrinsic origin of RT-FM in as-implanted film. However, substitution of Ni ions at tetrahedral Zn sites and oxygen vacancies as evident in O K-edge spectra of as-implanted film clearly indicate that clustering of TM cannot be the only source of observed RT-FM. The implantation of Ni in ZnO matrix creates oxygen vacancy related lattice defects as explained in our earlier works.[17,21,37,38] It is known that atomic defects in ionic crystals such as oxygen vacancies with trapped electrons form Hydrogen atom like structure. With increase in defect concentration, an impurity band is formed where electrons remain localized. Long range interaction of magnetic cations with hydrogenic electrons in the impurity band forms the bound magnetic polaron (BMP) structure.[39] BMPs starts overlapping and leads to BMP percolation after certain critical defect and magnetic cation density. Our experimental results at Ni and O K-edges for as-implanted film clearly show that oxygen vacancy defect constituted BMPs and Ni metal clusters are jointly responsible for the origin of RT-FM. The observed small saturation magnetization M_s in as-implanted film can be explained; as there are some of Ni ions in non-stoichiometric NiO phase outside these polarons, which may reduce the net magnetic moment as expected from BMP model as NiO is antiferromagnetic (AFM) with a Neel temperature T_N of 520 K.[40] However, for air annealed film, XANES study at O K-edge clearly indicates the absence/reduction of non-stoichiometric NiO phase and a significant enhancement in Ni^{2+} ion substitution at Zn^{2+} in tetrahedral environment. Within the BMP model, the greater substitution of Ni^{2+} ions at Zn^{2+} yields a greater volume occupied by BMPs. The greater density occupied by these BMPs increases the contribution of intrinsic component in observed saturation magnetization M_s, whereas Ni metal clustering appears similar in both films as suggested by Ni K-edge spectra. Therefore, enhancement in ferromagnetic contribution of air annealed film is explained on the basis of greater contribution from overlapping BMPs as compared to extrinsic Ni metal cluster.

IV. CONCLUSION

The PLD grown ZnO:Ni as-implanted and ZnO:Ni air annealed films do not show any crystalline phase corresponding to Ni or its oxide and exhibit RT-FM properties. The spectroscopic measurements show partial segregation of Ni metal in both the films and formation of non-stoichiometric NiO in as-implanted film and its absence/reduction in air annealed film. Apart from these observations, presence of oxygen vacancies in both films and substitution of Ni^{2+} ions at Zn sites with appreciable concentration in air annealed film was also evident. The absence of non-stoichiometric NiO secondary phase and greater number of BMPs in ZnO:Ni air annealed film leads to higher M_s even though there is partial clustering of Ni metal. RT-FM in ZnO:Ni as-implanted film does not disappear upon annealing in air at high temperature and found to be robust. Future studies should aim to decouple intrinsic and extrinsic origins for better understanding of the mechanism of FM in these magnetic materials.

ACKNOWLEDGMENTS

Authors (P.S. and S.G.) acknowledge the financial support from the Department of Science & Technology (DST), New Delhi, India, to carry out this work. One of the authors

(P. Satyarthi) is thankful to University Grants Commission (UGC), New Delhi, for the financial support through fellowship. K.A. acknowledges the Department of Physics, Tamkang University, Taiwan, for travel support to carry out measurements at NSRRC, Taiwan.

[1]H. Ohno, Science **281**, 951 (1998).
[2]S. J. Pearton, D. P. Norton, M. P. Mil, A. F. Hebard, J. M. Zavada, W. M. Chen, and I. A. Buyanova, IEEE Trans. Electron Devices **54**, 1040 (2007).
[3]K. Rode, A. Anane, R. Mattana, J. P. Contour, O. Durand, and R. LeBourgeois, J. Appl. Phys. **93**, 7676 (2003).
[4]M. Venkatesan, C. B. Fitzgerald, J. G. Lunney, and J. M. D. Coey, Phys. Rev. Lett. **93**, 177206 (2004).
[5]A. C. Tuan, J. D. Bryan, A. B. Pakhomov, V. Shutthanandan, S. Thevuthasan, D. E. McCready, D. Gaspar, M. H. Engelhard, J. W. Rogers, Jr., K. Krishnan, D. R. Gamelin, and S. A. Chambers, Phys. Rev. B **70**, 054424 (2004).
[6]X. Liu, F. Lin, L. Sun, W. Cheng, X. Ma, and W. Shi, Appl. Phys. Lett. **88**, 062508 (2006).
[7]W. Yu, L. H. Yang, X. Y. Teng, J. C. Zhang, Z. C. Zhang, L. Zhang, and G. S. Fu, J. Appl. Phys. **103**, 093901 (2008).
[8]S. Zhou, K. Potzger, J. von Borany, R. Grötzschel, W. Skorupa, M. Helm, and J. Fassbender, Phys. Rev. B **77**, 035209 (2008).
[9]M. Snure, D. Kumar, and A. Tiwari, Appl. Phys. Lett. **94**, 012510 (2009).
[10]Q. Xu, H. Schmidt, S. Zhou, K. Potzger, M. Helm, H. Hochmuth, M. Lorenz, A. Setzer, P. Esquinazi, C. Meinecke, and M. Grundmann, Appl. Phys. Lett. **92**, 082508 (2008).
[11]D. Gao, Z. Zhang, J. Fu, Y. Xu, J. Qi, and D. Xue, J. Appl. Phys. **105**, 113928 (2009).
[12]S. Banerjee, M. Mandal, N. Gayathri, and M. Sardar, Appl. Phys. Lett. **91**, 182501 (2007).
[13]X. J. Liu, X. Y. Zhu, C. Song, F. Zeng, and F. Pan, J. Phys. D: Appl. Phys. **42**, 035004 (2009).
[14]Z. Yin, N. Chen, F. Yang, S. Song, C. Chai, J. Zhong, H. Qian, and K. Ibrahim, Solid State Commun. **135**, 430 (2005).
[15]A. Ney, M. Opel, T. C. Kaspar, V. Ney, S. Ye, K. Ollefs, T. Kammermeier, S. Bauer, K.-W. Nielsen, S. T. B. Goennenwein, M. H. Engelhard, S. Zhou, K. Potzger, J. Simon, W. Mader, S. M. Heald, J. C. Cezar, F. Wilhelm, A. Rogalev, R. Gross, and S. A. Chambers, New J. Phys. **12**, 013020 (2010).
[16]A. Ney, K. Ollefs, S. Ye, T. Kammermeier, V. Ney, T. C. Kaspar, S. A. Chambers, F. Wilhelm, and A. Rogalev, Phys. Rev. Lett. **100**, 157201 (2008).
[17]P. Srivastava, S. Ghosh, B. Joshi, P. Satyarthi, P. Kumar, D. Kanjilal, D. Buerger, S. Zhou, H. Schmidt, A. Rogalev, and F. Wilhelm, J. Appl. Phys. **111**, 013715 (2012).
[18]J. Iqbal, B. Wang, X. Liu, D. Yu, B. He, and R. Yu, New J. Phys. **11**, 063009 (2009).
[19]L. N. Tong, X. M. He, H. B. Han, J. L. Hu, A. L. Xia, and Y. Tong, Solid State Commun. **150**, 1112 (2010).
[20]R. K. Singhal, S. C. Sharma, P. Kumari, S. Kumar, Y. T. Xing, U. P. Deshpande, T. Shripathi, and E. Saitovitch, J. Appl. Phys. **109**, 063907 (2011).
[21]B. Pandey, S. Ghosh, P. Srivastava, P. Kumar, D. Kanjilal, S. Zhou, and H. Schmidt, J. Appl. Phys. **107**, 023901 (2010).
[22]P. Kumar, G. Rodrigues, D. Kanjilal, A. Roy, B. P. Singh, and R. Kumar, Nucl. Instrum. Methods Phys. Res. B **246**, 440 (2006).
[23]J. F. Ziegler, J. P. Biersack, and U. Littmark, *The Stopping Power of Ions in Solids* (Pergamon, New York, 1980).
[24]K. Potzger, S. Zhou, H. Reuther, A. Mucklich, F. Eichhorn, N. Schell, W. Skorupa, M. Helm, J. Fassbender, T. Hermannsdorfer, and T. P. Papageorgiou, Appl. Phys. Lett. **88**, 052508 (2006).
[25]S. Zhou, K. Potzger, G. Talut, J. von Borany, W. Skorupa, M. Helm, and J. Fassbender, J. Appl. Phys. **103**, 07D530 (2008).
[26]J. C. A. Huang, H. S. Hsu, Y. M. Hu, C. H. Lee, Y. H. Huang, and M. Z. Lin, Appl. Phys. Lett. **85**, 3815 (2004).
[27]H. S. Hsu, J. C. A. Huang, Y. H. Huang, Y. F. Liao, M. Z. Lin, C. H. Lee, J. F. Lee, S. F. Chen, L. Y. Lai, and C. P. Liu, Appl. Phys. Lett. **88**, 242507 (2006).
[28]X. Wang, L. Zhu, L. Zhang, J. Jiang, Z. Yang, Z. Ye, and B. He, J. Alloys Compd. **509**, 3282 (2011).
[29]V. Ney, S. Ye, T. Kammermeier, K. Ollefs, A. Ney, T. C. Kaspar, S. A. Chambers, F. Wilhelm, and A. Rogalev, J. Magn. Magn. Mater. **322**, 1232 (2010).
[30]J. A. Bearden and W. W. Beeman, Phys. Rev. **58**, 396 (1940).
[31]T. C. Kaspar, T. Droubay, S. M. Heald, M. H. Engelhard, P. Nachimuthu, and S. A. Chambers, Phys. Rev. B **77**, 201303 (R) (2008).
[32]P. Thakur, V. Bisogni, J. C. Cezar, N. B. Brookes, G. Ghiringhelli, S. Gautam, K. H. Chae, M. Subramanian, R. Jayavel, and K. Asokan, J. Appl. Phys. **107**, 103915 (2010).
[33]S. Krishnamurthy, C. McGuinness, L. S. Dorneles, M. Venkatesan, J. M. D. Coey, J. G. Lunney, C. H. Patterson, K. E. Smith, T. Learmonth, P. A. Glans, T. Schmitt, and J. H. Guo, J. Appl. Phys. **99**, 08M111 (2006).
[34]Z. Sun, W. Yan, G. Zhang, H. Oyanagi, Z. Wu, Q. Liu, W. Wu, T. Shi, Z. Pan, P. Xu, and S. Wei, Phys. Rev. B **77**, 245208 (2008).
[35]I. Preda, M. Abbate, A. Gutierrez, S. Palacin, A. Vollmer, and L. Soriano, J. Electron Spectrosc. Relat. Phenom. **156**, 111 (2007).
[36]X. Zhao, E. Liu, R. V. Ramanujan, and J. Chen, Curr. Appl. Phys. **12**, 834 (2012).
[37]B. Pandey, S. Ghosh, P. Srivastava, P. Kumar, and D. Kanjilal, J. Appl. Phys. **105**, 033909 (2009).
[38]S. Ghosh, D. Kanjilal, B. Pandey, M. Saurav, and P. Kumar, Radiat. Eff. Defects Solids. **163**, 215 (2008).
[39]J. M. D. Coey, M. Venkatesan, and C. B. Fitzgerald, Nature Mater. **4**, 173 (2005).
[40]D. A. Schwartz, K. R. Kittilstved, and D. R. Gamelin, Appl. Phys. Lett. **85**, 1395 (2004).